Egypt. J. Chem. **Vol. 68,** SI: Z. M. Nofal, pp. 365- 380 (2025)

Egyptian Journal of Chemistry

http://ejchem.journals.ekb.eg/

Metabolic profiling of *Lagunaria patersonii* leaves extract in relation to its cytotoxic activity: *in vitro* and *in silico* studies

Mayar M. Eladl [*1], Mahmoud T. Abo-Elfadl[2], Ahmed A. Al-Karmalawy [3,4], Osama G. Mohamed [1,5] , Ashootosh Tripathi [5,6], Nabaweya M. El-Fiky [1],Nabil M. Selim [1 #], Amira K. Elmotayam [1 #].

[1] *Pharmacognosy Department, Faculty of Pharmacy, Cairo University, Cairo 11562, Egypt*
[2] *Biochemistry Department, Biotechnology Research Institute, Cancer Biology and Genetics Laboratory, Centre of Excellence for Advanced Sciences, National Research Centre, Giza 12622, Egypt.*
[3]*Department of Pharmaceutical Chemistry, College of Pharmacy, The University of Mashreq, Baghdad 10023, Iraq.*
[4] *Department of Pharmaceutical Chemistry, Faculty of Pharmacy, Horus University-Egypt, New Damietta 34518, Egypt.*
[5]*Natural Products Discovery Core, Life Sciences Institute, University of Michigan, Ann Arbor, MI 48109, USA,*
[6]*Department of Medicinal Chemistry, College of Pharmacy, University of Michigan, Ann Arbor, MI 48109, USA, # Both authors contributed equally.*

Abstract

Lagunaria patersonii(Andrews) G. Don. leaves were studied for their cytotoxic activity in relation to phytoconstituents on different tumor cell lines. The fractions prepared from the total alcoholic extract: n-hexane (Hex.), dichloromethane (DCM), ethyl acetate (EtOAc), and butanol (BuOH) were evaluated on three human cancer cell lines: Caco-2, MCF7, and PC3, using MTT assay. Both Hex and DCM showed strong cytotoxic activity against PC3 cells and moderate cytotoxic activity against Caco-2 and MCF7 cell lines. Thus, the fluorescent staining and immunofluorescence techniques were used to determine the effects of Hex and DCM fractions on cell death and the anti-apoptotic protein (BCL-2) expression in PC3 cells. The predominant mode of cell death was late apoptosis. Meanwhile, there was a significant decrease in BCL-2 protein expression in both Hex and DCM-treated cells compared to untreated control cells. The two bioactive fractions were screened for their phytoconstituents using UHPLC-QTOF-MS/MS where 22 compounds were tentatively identified. In addition, the Hex fraction was examined using GLC for its lipid content. 33 fatty acids were detected in the saponifiable fraction, while 19 compounds were detected in the unsaponifiable fraction. The isolated bioactive compounds from the two fractions were identified as 24-methylene-3, 4-seco-cycloart-4(28)-en-3-oic acid, triolein, and stigmasterol. A molecular docking study on BCL-2 target receptor revealed that the isolated compounds demonstrated high binding scores, particularly triolein, which surpassed the co-crystallized ligand. This strongly suggests the significant apoptotic potential of the examined candidates derived from Lagunaria patersonii (Andrews) G. Don leaves.

Keywords: Apoptosis; MTT assay; 24-methylene-3, 4-seco-cycloart-4(28)-en-3-oic acid; Molecular docking, *Lagunaria patersonii*,BCL-2, PC3 cell line

Introduction

Cancer is a disease characterized by the uncontrolled growth and spread of abnormal cells that can invade and damage surrounding tissues [1]. It can affect people of all ages, but the risk of cancer increases with age. Most cancers are caused by a combination of lifestyle and environmental factors, such as tobacco use, unhealthy diet, lack of physical activity, exposure to radiation, pollution, and infectious agents [2]. However, some cancers are caused by genetic mutations that can be inherited from parents. It is estimated that 5-10% of all cancers are caused by inherited genetic mutations [3].

The use of alternative therapies, such as medicinal plants and herbal medicines, has increased worldwide due to their lower cost and less toxic effects compared to conventional medicines [4] Furthermore, herbal medicines have a significant impact on both global health and international trade, especially in developing countries where they have a long and uninterrupted history of use. In addition, they are more culturally and spiritually acceptable [5]. Natural products remain an

*Corresponding author e-mail: mayar.eladl@pharma.cu.edu.eg.; (**Mayar M. Eladl**).
Received date 05 April 2025; Revised date 18 May 2025; Accepted date 02 June 2025
DOI: 10.21608/EJCHEM.2025.372647.11547

inexhaustible source of powerful anti-cancer drugs. Studies have shown that most phytochemicals interfere with several cell-signaling pathways, leading to cell cycle arrest and/or differentiation induction, as well as their ability to induce apoptosis [6].

Apoptosis is a fundamental process that plays a crucial role in maintaining tissue homeostasis in all organ systems in the human body [7].

It is important to note that most cell death is an active process initiated by specific signals. There are three primary categories of cell death, largely categorized based on the morphological characteristics of the dying cell: apoptosis (type I cell death), autophagic cell death (type II), and necrosis (type III) [8]. Two families of genes are likely to be crucial in the control of apoptosis. The first is the gene family encoding the interleukin-1beta-converting enzyme family of cysteine proteases, and the second is the gene family associated with the proto-oncogene BCL-2. Both gene families share homology with cell death genes found in *C. elegans*. In mammalian cells, the number of identified members within both gene families is rapidly increasing. Considerable efforts are being made to define the functions of each organelle and understand how they interact to control programmed cell death [9].

Nowadays, computational studies (such as molecular docking) have become a crucial cornerstone in the drug discovery process. It saves time, effort, and money to predict the target receptor/s and/or investigate the proposed biological activity of the target candidate/s [10, 11].

Genus *Lagunaria* belonging to the family Malvaceaeconsists of two species*: Lagunaria patersonii* (Andrews) G. Don., and *Lagunaria queenslandica* craven (Lagunaria (A.DC.). *L. patersonii* is the only species cultivated in Egypt. *L. patersonii*traditionally used for fibers in fishing gear. Its fruits and seeds are known to contain polyphenols, flavonoids, and various fatty acids, including oleic, palmitic, malvalic, sterculic, and traces of dihydrosterculic acid. To our knowledge, few reports have been traced on the biological activity of the plant including insecticidal [12] and antioxidant activities [13].

Malvaceae plants are widely recognized as important icons of the tropics and subtropics and have a prominent economic and therapeutic reputation. They are commonly used as ornamental plants, as folk remedies, and as a source of food and fiber [14]. Studies on plant-derived products in the treatment of cancer have mainly focused on some common species of Malvaceae family such as *Sida acuta, Bombax ceiba, Malva sylvestris, Hibiscus sabdariffa* and *H. rosa-sinesis*that have showed significant cytotoxic activity in different studies [15-17],[18],[19]. While many other species of the family have received less attention, including *L.patersonii.* There is no study available in the literature regarding the cytotoxic activity of the plant, so the current study aimed to investigate the cytotoxic activity of the different fractions of *L. patersonii* leaves together with comprehensive chemical profiling using UHPLC-QTOF-MS/MS, gas-liquid chromatography (GLC) and isolation of the major compounds. Molecular docking was performed on specific target receptor to evaluate the apoptotic activity of the identified and isolated compounds from *L. patersonii*leaves.

Experimental

Collection and identification

The leaves of *L. patersonii* were collected from the private garden ″El-Abd Botanical Garden ″ (Cairo Alex. Desert Road, Egypt) in January 2022. The plant was authenticated and confirmed by Ms Therese Labib, Botanical Specialist and Consultant at Orman and Qubba Botanical Gardens & Prof. Dr. Reem Samir Hamdy, Professor of Plant Taxonomy and Flora, Faculty of Science, Cairo University. A voucher specimen (No. 27.02.2022I) was kept at the herbarium of the Department of Pharmacognosy, Faculty of Pharmacy, Cairo University.

Extraction and fractionation

The air-dried powdered leaves (2.866 kg) were extracted by repeated maceration in cold 70% ethanol (5 times) till exhaustion followed by filtration. The filtrates were combined and evaporated under reduced pressure (40 °C) in a rotary evaporator (Büchi, Switzerland) to give 330 g greenish-black dried residue. An aliquot (280 g) of theethanol extract was suspended in distilled water followed by fractionation with Hex., DCM, EtOAc, and BuOH saturated with water. The solvent of each fraction was distilled off, and the obtained residue was dried and weighed 26.771 g, 8.077 g, 5.0964 g, and 24.4268 g, respectively.

In vitro screening of cytotoxic activity

Cell lines

Human epithelial-like large intestine colorectal adenocarcinoma, Caco-2 cell line; human epithelial breast adenocarcinoma, MCF7 cell line; and human epithelial prostate adenocarcinoma, grade IV, PC3 cell line were all purchased from the American Type Cell Culture (ATCC, USA). All cell lines were routinely cultured in a high glucose Dulbecco's Modified Eagle Medium (DMEM), supplemented with 10% fetal bovine serum (FBS), and 2 mM L-glutamine, in addition to 1% antibiotic and antifungal cocktail. All from Lonza, (Basel, Switzerland). Cells were maintained at a sub-confluent temperature of 37ºC in humidified air containing 5% CO_2. For sub-culturing, monolayer cells were harvested after trypsin/EDTA treatment at 37°C. Cells were used when confluence had reached 75%.

Chemicals and reagents

All solvents and reagents used for extraction, fractionation, and isolation of compounds were of analytical grade. Organic solvents were purchased from El-Nasr Company for chemicals, Cairo, Egypt.Solvent systems for TLC: S1 (hexane and methylene chloride in a 95:5 volume ratio), S2 (hexane and ethyl acetate in a 90:10 volume ratio), and S3 (hexane and ethyl acetate in an 80:20 volume ratio). *p*-Anisaldeyde reagent was prepared according to Stahl et.al [20].

Cytotoxic screening of plant fractions

Cellular proliferation assay

The cytotoxicity of the tested fractions against Caco-2, MCF-7, and PC3 cell lines was measured using MTT cell viability assay [21]. Briefly, cells ($0.5X10^5$ cells/ well), in serum-free media were plated in a flat bottom 96-well microplate and treated with 20 µl of various fractions concentrations for 48 h at 37º C, in a humidified 5% CO_2 atmosphere. The concentration used ranged from 100 µg/ml to 3.125 µg/ml. After incubation, the media was removed and 40 µl MTT solution / well was added and incubated for an additional 4 h. MTT crystals were solubilized by adding 180 µl of acidified isopropanol / well and the plates were shacked at room temperature, followed by photometric determination of the absorbance at 570 nm using microplate ELISA reader (FLUOstar OPTIMA, BMG LABTECH, Ortenberg, Germany). Triplicates were performed for each concentration and the average was calculated. Data were expressed as the percentage of relative viability compared with the untreated cells compared with the vehicle control and with cytotoxicity indicated by <100% relative viability. The viability percentage was calculated by comparing the values obtained from the control with those obtained from different treatments. The half-maximal inhibitory concentration (IC_{50}) then was calculated from the dose-response curve equation.

Mode of cell death detection

Using fluorescence staining technique to detect cell death mode, PC3 cells were cultured on 8 well cell culture slides (SPL, Seoul, South Korea) at a density of 10^4 cells / well, and samples were adjusted to a final concentration of half the IC_{50} of the samples. Cells were left for 48 h. The mode of cell death was investigated after staining with acridine orange (100 µg/ml) and ethidium bromide (100 µg/ml) dissolved in phosphate buffer saline (PBS) in equal volume. All reagents were obtained from Merck KGaA (Darmstadt, Germany). Cells were stained and examined under a fluorescent microscope (AxioImager Z2, Zeiss, Jena, Germany). Green-stained cells were recorded as live cells, and yellow, orange, or red-stained cells were recorded as early, late, or necrotic cells, respectively [22]. The experiments were repeated three independent times.

BCL-2 protein expression detection

PC3 cells were cultured on 8 well cell culture slides (SPL, Seoul, South Korea) at a density of 10^4 cells / well, and ½ IC_{50} of the samples was added to each well separately. After 48 h. of incubation, cells were fixed with 4% paraformaldehyde and permeabilized with 0.1% tritonX-100. Cells were then blocked with 1% bovine serum albumin for one hour and incubated overnight at 4ºC with the anti-BCL-2 antibody ab59348 (Abcam, Cambridge, United Kingdom) at a dilution of 1/500. After 3 repeats of PBS wash, cells were incubated at room temperature for 1 h with the secondary antibody goat anti-rabbit IgG (Alexa Fluor®488) ab150077 (Abcam, Cambridge, United Kingdom) at 1/1000 dilution. After 3 repeats of PBS washing and air drying, glycerol mounting medium with DAPI (ab188804, Abcam, Cambridge, United Kingdom) was used as an antifade and as a counterstain for nuclei. Cells were then imaged under an AxioImager Z2 fluorescent microscope (Zeiss, Jena, Germany) and fluorescence intensity was measured using Zen11 Blue edition software (Zeiss, Jena, Germany) [23].

Statistics

Data are presented as mean ± SD. The dose-response curve was calculated using non-linear regression analysis with 5 parametric logistic curve equations, total fraction, and ordinary one-way ANOVA with Tukey's for multiple comparison tests between groups were performed using GraphPad Prism 9.4.1 (458) for MacOS, GraphPad Software, (San Diego, California USA, www.graphpad.com).

UHPLC/Q-TOF-MS/MS profiling of the biologically- active fractions

The different components of the most active fractions were identified using ultra-high-performance liquid chromatograms (UHPLC), acquired on an Agilent LC–MS system consisting of an Agilent 1290 Infinity II UHPLC coupled to an Agilent 6545 ESI-Q-TOF-MS in negative mode, and aliquots (1 µl) of the fractions (0.5 mg/ml in MeOH) were analyzed on a Kinetex phenyl-hexyl column (1.7 µm, 2.1 × 50 mm) and eluted with 1 min isocratic elution of 90% A (A: 100% H_2O + 0.1% formic acid) followed by 6 min linear gradient elution to 100% B (95% MeCN + 5% H_2O + 0.1% formic acid) at a flow rate of 0.4 ml/min. ESI conditions were set as described in [24]. The .mzXML files were imported and processed using MZmine 2 v2.53 [25]. The resulting feature lists were exported to the GNPS-compatible format, using built-in custom "Export for GNPS" options.

Preparation of the unsaponifiable matters and fatty acid methyl esters

The Hex fraction of the air-dried *L.patersonii*leaf powder was subjected to alkaline hydrolysis by alcoholic potassium hydroxide to give unsaponifiable and saponifiable matters then kept in a desiccator for analysis by GLCaccording to (Vogel et al. and Farag et al.)[26],[27].

GLC of unsaponifiable matters

The column used was HP-5 (film thickness 30 m × 0.32 mm × 0.25 μm), packed with (5% phenyl methyl siloxane). The injected volume was 2 μl. The analysis was performed at a programmed temperature. The initial temperature was 80°C, held constant for 1 min, then increased to 300 °C at a rate of 8°C/min, then maintained isothermal for 20 min. The injector temperature was 240 °C and the detector temperature was 280 °C. Nitrogen was used as the carrier gas at a flow rate of 24 ml/min. FID detector was used.

GLC of fatty acid methyl esters

The analysis was performed on an Agilent Technologies Inc HP-5 GC column, the same column dimensions as used for unsaponifiable matter with the same injection volume, flow rate, injector temperature, detector, and carrier gas. However,

the initial temperature was 70°C for 1 min. and the final temperature was 190°C for 20 min. The detector temperature was 300 °C.

Isolation of the main compounds from the bioactive fractions

The Hex fraction of the leaves was saponified, and a portion of the unsaponifiable matter (450 mg) was purified by repeated silica column chromatography using 100% Hex followed by Hex/EtOAc with 10% increased polarity. Fractions with the same pattern on TLC were pooled together and concentrated to yield, compound I, a white amorphous powder (9 mg). and showed a purple spot on TLC (Rf = 0.711 in S3) when sprayed with p-anisaldehyde/H_2SO_4. Another portion of the unsaponifiable material was fractionated by VLC (vacuum liquid chromatography) using gradient elution. Similar fractions were pooled together, purified, and concentrated yielding compound 2, a white amorphous powder (12 mg) showing a purple spot on TLC (Rf = 0.56 in S3) when sprayed with p-anisaldehyde/H_2SO_4.

The DCM fraction (7gm) was fractionated using VLC. Gradient elution was performed by Hex., DCM, EtoAC and MeOH. Fractions with the same pattern on TLC were collected. Specific pooled fractions with a major spot were weighed (1.2 g) and fractionated on silica column chromatography using 98% Hex.:2%EtoAC with 2% increment in polarity. Subfractions were monitored by TLC and pooled together, further purification with silica column was done for certain pooled subfractions using 97% Hex.:3% EtoAC with 2% increment in polarity, yielding white needles (10mg), showing one major blue spot (Rf = 0.51 in S3) after spraying with p-anisaldehyde/H_2SO_4.

Docking studies

AutoDock Vina and PyMol[28, 29]were applied to evaluate the apoptotic potential of the identified and isolated compounds from *L.patersonii*towards the BCL-2 receptor. The structures of twenty identified and three chemically isolated compounds were generated in the ChemDraw and transferred for preparation by energy minimization and partial charges optimization.[30]. Furthermore, the target BCL-2 receptor was downloaded from the Protein Data Bank (ID: 4C5D). It was corrected, energy minimized, and 3D hydrogenated as well.[31] Finally, a redocking process of the co-crystallized ligand of the BCL-2 receptor within its binding pocket was applied to validate the software. A low RMSD value (<2 Å) and comparable binding mode indicate correct performance [32].

Results and discussion

Prostate cancer is recognized as a leading cause of death among men worldwide. Several medicinal plants have been found to induce apoptosis in cancer cells, offering therapeutic potential. Therefore ongoing research in alternative medicine is focused on exploring the beneficial properties of these plants to develop new anticancer drugs [33]. Traditional medicine has always been an important source of effective drugs introduced to the international pharmaceutical market. People, particularly in developing countries, use herbal medicines to treat a wide range of ailments. They believe that, apart from being available and affordable, the side effects of these natural drugs are less than those of synthetic ones. An ideal anticancer drug should target and kill cancer cells without affecting normal cells. In this regard, inducing apoptosis in cancer cells is the optimal strategy [34]. The world is currently facing an increasing number of cancer patients, making cancer the second cause of death after cardiac diseases. Therefore, understanding the mechanisms underlying cancer pathogenesis is crucial for developing new therapeutic approaches [35].

Cytotoxic assay

The cytotoxic activity was assessed for the four fractions across the normal retinal pigment epithelial cell (RPE1) and three distinct cell lines, namely Caco-2, MCF7, and PC3 (Figures 1 and 2). The IC_{50} values were determined, revealing that the most favorable results were observed in the PC3 cell line for both hexane and DCM fractions (**Table 1**).

Table 1: IC_{50} values for (Hex., DCM, EtOAC, and BuOH) fractions of *Lagunaria patersonii* leaves extract across normal and different cancer cell lines (*µ*g/ml)

Cell line	Hex.	DCM	EtOAC	BuOH
RPE1	96.0 ± 7	56.5 ± 4	114.3± 10	--
Caco-2	96.29 ± 38.94	101.2 ± 16.865	--	--
MCF-7	85.49 ± 27.66	64.65 ± 26.815	105.7± 28.14	94.60± 17.49
PC3	55.50 ± 7.68	43.07 ± 7.25	81.46± 12.19	--

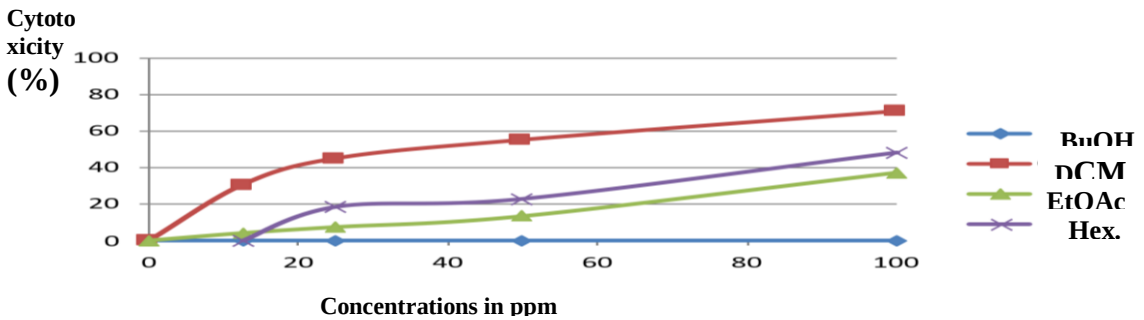

Figure 1: Cytotoxicity of different fractions of *L. patersonii* on normal retinal pigment epithelial cell (RPE1) cell line**.**

Figure 1, illustrating the effect of the 4 fractions on normal cell line, concerning the safety of the fractions: BuOH> EtOAC > Hex > DCM where BuOH is the safest one. Selectivity index for the fractions was calculated according to the following equation SI: IC_{50}(normal cells)/IC_{50}(malignant cell). The results revealed that BuOH fraction was highly selective on cancer cells selectivity index >3, while hex. fraction has intermediate selectivity, especially for the PC3 cell line selectivity index >1.5 (**Table 2**).

Table 2: selectivity index for the fractions of *Lagunaria patersonii* leaves extract across different cell lines.

Cell line	Hex.	DCM	EtOAC	BuOH
Caco-2	0.997	0.558	--	>3
MCF-7	1.123	0.874	1.081	>3
PC3	1.73	1.312	1.403	>3

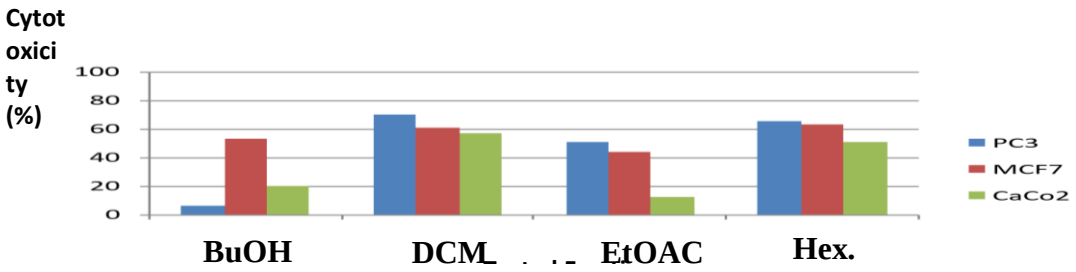

Figure 2: Cytotoxicity of different fractions of *L. patersonii* on 3 cancer cell linesat 100 ppm.

Fluorescing staining technique:

Using the AC/EtBr fluorescent stain to detect the cell death modes, the photos showed that apoptosis was induced significantly in cells treated with Hex. and DCM compared to the untreated control cells. Both early and late apoptosis were induced in treated cells in addition to valuable necrotic cells. Late apoptosis was seen predominantly in the DCM-treated cells with an increased necrosis ratio in comparison to the Hex-treated cells. The illustrative photos and cell death mode distributions are shown in **Figure 3.**

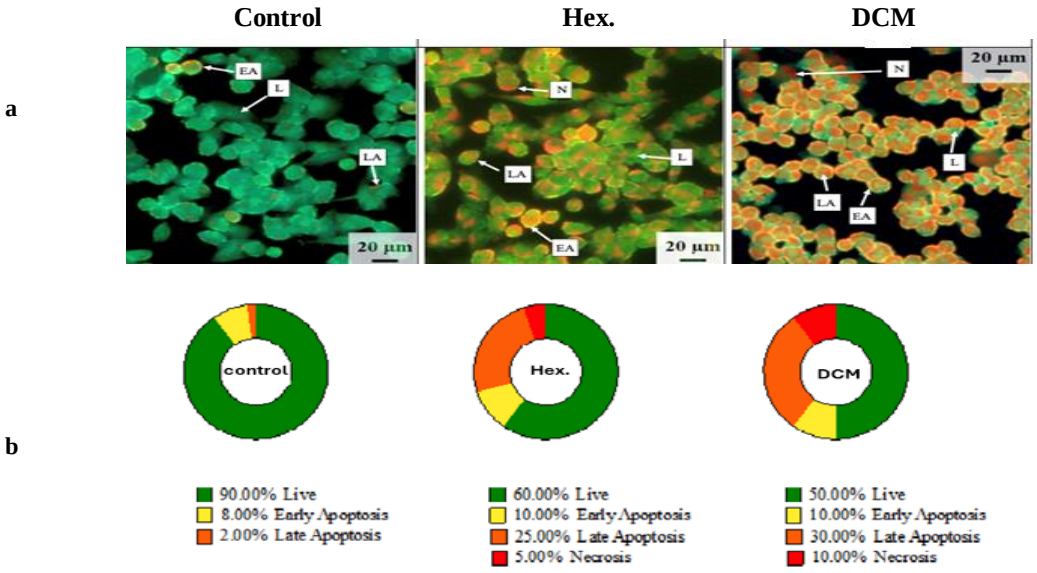

Figure 3: Mode of cell death of PC3 cells after treatment with Hex. and DCM samples at their respective ½ IC_{50}. **(a)** the fluorescent photos using AO/EtBr stain. The photos show live cells (L), early apoptotic cells (EA), late apoptotic cells (LA), and necrotic cells (N). The magnification is 20X and the scale bar is 20 µm. **(b)** The distribution of cell death modes in each sample was measured by Zen 11 blue edition software. Late apoptosis is abundant in both Hex. and DCM samples compared to the control cells. There is also a valuable necrosis percentage in both Hex. and DCM. The data are based on 1000 cells/ sample, n=3.

Immunofluorescence assay.

Using the immunofluorescence technique to detect the BCL-2 protein expression in the Hex. and DCM treated cells, the photos showed a significant decrease in the BCL-2 protein expression in both Hex. and DCM treated cells in comparison to the untreated control cells, $p< 0.001$. On the other hand, there was no significant difference in the BCL-2 protein expression among Hex. and DCM-treated cells, $p> 0.05$. **Figure 4** illustrates the immunofluorescent photos of BCL-2 protein expression and the expression % difference among Hex., DCM, and control cells.

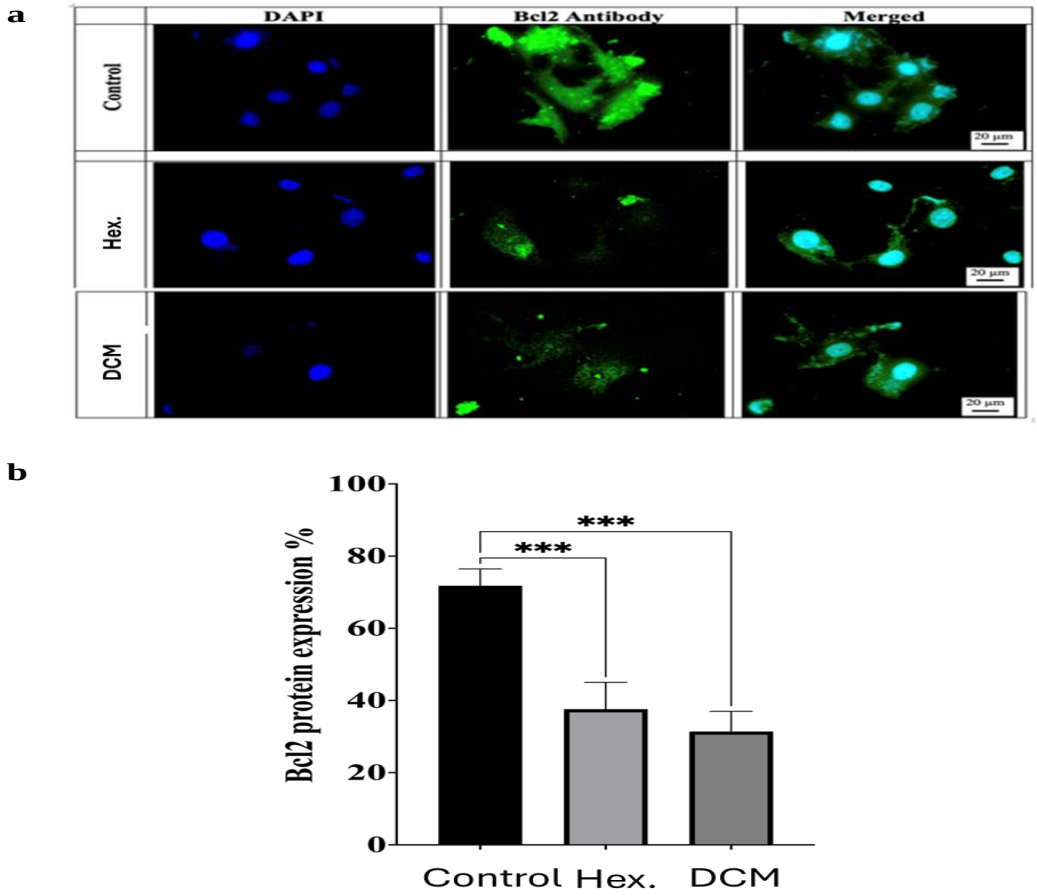

Figure 4: The Bcl2 protein expression in PC3 cells after treatment with Hex. and DCM samples at their respective ½ IC_{50}. **(a)** the immunofluorescent photos show high expression of Bcl2 protein in control cells while low expression in both Hex. and DCM treated cells. The magnification is 40X and the scale bar is 20 µm. **(b)** the protein expression % in treated cells compared to the control using One-way ANOVA, the data shows significant high expression in the control cells compared to both the Hex. and DCM treated cells ($p< 0.001$). There is no significant difference in protein expression between Hex. and DCM ($p> 0.05$). The data are based on 1000 cells/ sample, n=3.

Interpretation

Both Hex. and DCM fractions induced apoptosis in PC3 cells. The prevalent mode of cell death was late apoptosis. The early apoptosis and necrosis modes were also observed in significant percentages in treated cells when compared to the untreated control cells. This was further supported by measuring the expression of anti-apoptosis protein; BCL-2 by immunofluorescence technique. The inhibition of the BCL-2 protein in cancer cells promotes apoptosis and consecutive cell death [36].

UHPLC-QTOF-MS/MS profiling of the bioactive fractions of *L. patersonii*.

The Hex.and DCM fractions of *L. patersonii* leaves were analyzed using UHPLC-QTOF-MS/MS in negative mode. Molecular formula prediction and peak identification were performed with various databases and software, identifying 22 compounds including 10 fatty acids, 5 flavonoids, 3 lipids, 2 phenolic acid ,1 sterol and 1 hydroxy coumarin. Table 3 lists the metabolites, retention times, *m/z* ratios of molecular and fragment ions, and projected molecular formulas. Total ion chromatograms are shown in **Figures 5** and **6**.

Table 3: Secondary metabolites of the bioactive fractions (Hex. and DCM) *of L. patersonii* leaves identified using UHPLC-Q-TOF-MS (negative mode).

No	R_t (min)	$(M-H)^-$	Molecular Formula	Error (ppm)	Identification	MS/MS	Class	Hex. fraction	DCM fraction	Ref.
1	1.33	307.1211	$C_{18}H_{28}O_4$	-0.38	Hydroxy-oxo-octadecatrienoic acid	289, 185	Fatty acid	-	+	[37]
2	2.89	447.0929	$C_{21}H_{20}O_{11}$	-0.8	Luteolin-6-C-hexoside	357, 327, 285, 133	flavone C-glycosides	-	+	[38]
3	2.91	623.1613	$C_{28}H_{32}O_{16}$	-0.7	Isorhamnetin-3-O-dihexoses	315, 271, 300, 255	flavonol 3-O glycosides	-	+	[39]
4	2.94	417.1038	$C_{17}H_{21}O_{12}$	0.12	Dihydroxybenzoic acid-O-dipentoside	153, 152, 109, 108	Phenolic acid	-	+	[40]
5	3.02	193.0499	$C_{10}H_9O_4$	4.35	Scopoletine	178, 133, 105	Hydroxy coumarin	-	+	[41]
6	3.57	593.1306	$C_{30}H_{26}O_{13}$	-0.2	Tiliroside	285, 284, 447	flavonol 3-O glycosides	-	+	[42]
7	3.60	327.217	$C_{18}H_{32}O_5$	-0.8	Malyngic acid	229, 211	fatty acid	-	+	[43]
8	3.74	329.233	$C_{14}H_{18}O_9$	-0.4	Vanillicacid hexoside	167, 329	Phenolic acid	-	+	[44]
9	3.82	183.1392	$C_{11}H_{20}O_2$	0.9	Dimethyl nonenoic acid	-	fatty acid	-	+	[45]
10	3.83	227.1291	$C_{12}H_{20}O_4$	1.1	Traumatic acid	-	fatty Acyls	-	+	[46]
11	3.91	299.0558	$C_{16}H_{12}O_6$	-1.0	Diosmetin	258, 153	flavone	-	+	[47]
12	4.27	311.1845	$C_{18}H_{31}O_4$	3.15	Dihydroxy-octadecadienoic acid	293, 275, 223	fatty acid	-	+	[48]
13	4.61	721.3645(2M adduct)	$C_{33}H_{55}O_{14}$	0.28	Dihexosyl-monoacyl glycerol (18:3)	415,397,277	lipids	+	-	[48]
14	4.79	577.2669	$C_{27}H_{45}O_{11}S$	0.7	Sulfoquinovosyl monoacyl glycerol (18:3)	277, 225	lipids	+	-	[48]
15	4.93	293.2107	$C_{18}H_{29}O_3$	1.08	Hydroxy-octadecatrienoic acid	275,231,185,171,121	fatty acid	+	-	[48]
16	5.07	555.2828	$C_{22}H_{19}O_{15}S$	0.39	"Iso"scutellarein 4′-methyl ether 8-(2″-sulfatoglucuronide)	494, 299	Flavonoids	+	-	[49]
17	5.08	555.2838	$C_{25}H_{47}O_{11}S$	1.18	Sulfoquinovosyl monoacyl glycerol (16:0)	255, 225	lipids	+	-	[48]
18	5.09	291.1951	$C_{18}H_{27}O_3$	0.11	Oxo-octadecatrienoic acid	185, 121	fatty acid	+	+	[50]
19	5.13	295.228	$C_{18}H_{33}O_3$	-9.6	13(S)-hydroxy octadecadienoic acid (α-artemisolic acid)	277, 195, 171	fatty acid	+	-	[51]
20	5.65	271.2273	$C_{16}H_{32}O_3$	-2.0	2-hydroxy palmitic acid	253, 225	fatty acid	+	+	[51]
21	5.85	277.2166	$C_{18}H_{30}O_2$	-2.4	Linolenic acid	234, 59	fatty acid	+	-	[52]
22	6.73	471.3827	$C_{31}H_{52}O_3$	-3.5	Theonellasterol D	293, 203	4-methylene-24-ethylsteroid	+	-	[53]

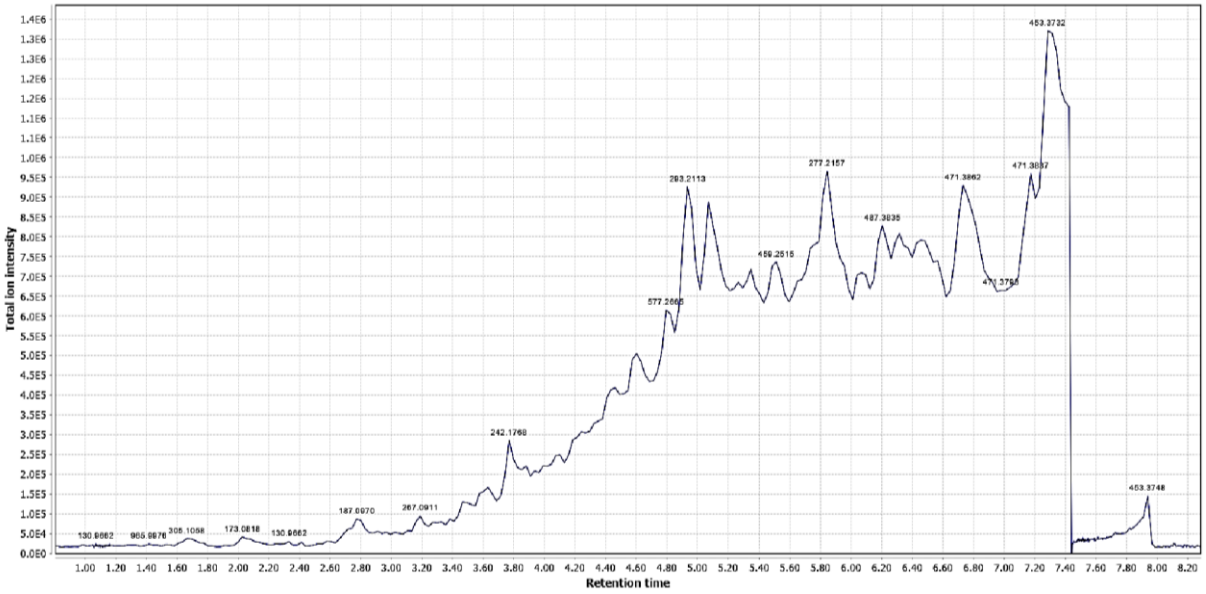

Figure 5: Total ion chromatogram of *L.patersonii* leaves of Hex. fraction in the negative ionization mode.

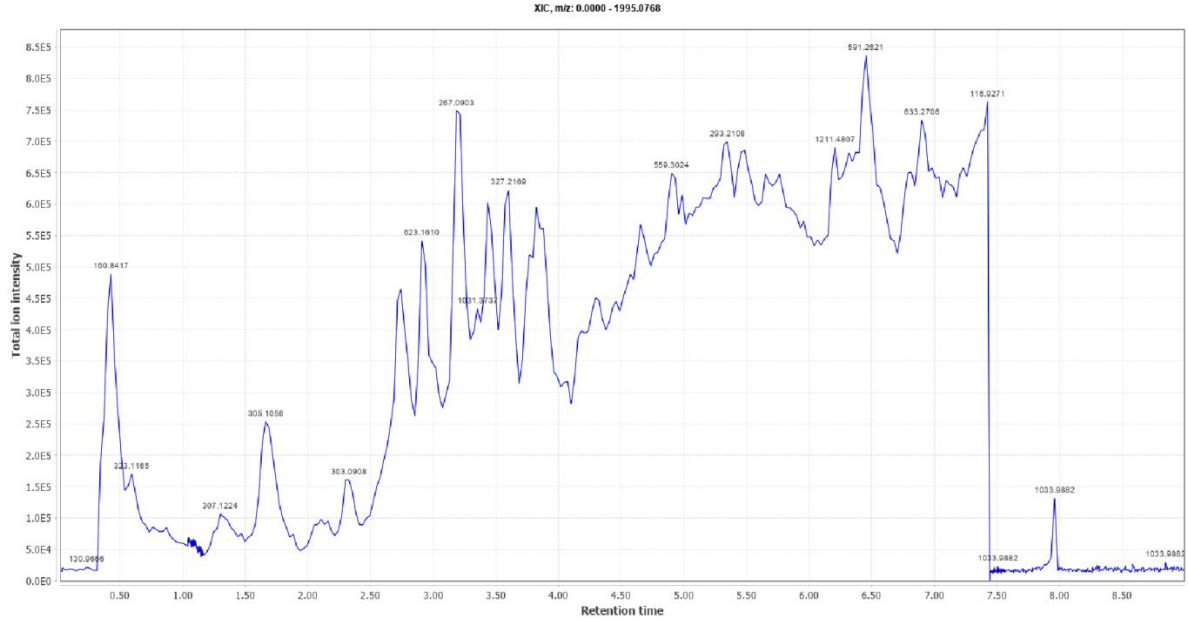

Figure 6: Total ion chromatogram of *L.patersonii* leaves of DCM fraction in the negative ionization mode.

Identification of flavonoids, phenolic acids and coumarins:

One flavone was identified at peak **11**, R_t (min) 3.91 with molecular ion peak [M-H] at *m/z* 299.0558 and fragment ion peaks at 258 and 153. The aforementioned aglycone was identified as diosmetin and was previously identified in different members of the family Malvaceae[54][55]. Compound **3** with R_t (min) 2.91 has a molecular ion peak (*m/z* 623.1613) where its aglycone moiety is represented in the product ion peak at *m/z* 315, fragment ion peaks 300 $[M\text{-}H\text{-isorhamnetin-}CH3]^-$,271 $[M\text{-}H\text{-isorhamnetin-}CH3\text{-}CHO]^-$.This compound was identified as isorhamnetin-3-O-dihexoside [54].

Compound **6** R_t (min) 3.57 with molecular ion peak at *m/z* 593.130, Fragments 447 [M-H- *p*-coumaroyl] $^-$, 285 [M-H- *p*-coumaroyl-glucosyl] $^-$ for kaempferol aglycone moiety. Compound **6** was identified as Kaempferol–3-O-β-D-(6″-*p*-coumaroyl)-glucopyranoside (tiliroside) [54],[56]. The fragmentation pattern of C- glycoside flavonoids was clearly observed in compound no.**2** showing molecular ion peak at *m/z* 447.0929, fragment ion peaks 357 $[M - H - 90]^-$,327 $[M - H - 120]^-$ characteristic for a hexose substitution in the aglycone moiety, 285 $[M - H - 162]^-$ for the aglycone moiety luteolin,133 by retro-Diels-Alder (RDA) cleavage.This compound is well known in the family Malvaceae and identified as Luteolin-6-C-hexoside [57], [58], [59]. Two phenolic acid glycosides could be traced in DCM fraction at peak **8** R_t (min) 3.74 identified as vanillic acid hexoxide producing a molecular ion peak at *m/z* 329.233 and a product ion peak at *m/z* 167(loss of hexose), corresponding to vanillic acid moiety. Compound **4** showed a molecular ion peak at *m/z* 417.1038. The molecular ion

fragmented to give fragment ions at *m/z* 285 [M – H - pentose]$^-$, 241 [M – H – pentose - CO2]$^-$, and 153 [M – H - 2 pentose]$^-$ corresponding to dihydroxybenzoic acid moiety. Compound **4** was identified as a Dihydroxybenzoic acid-O-dipentoside.

Identification of fatty acids, sterols and lipids:

Different plants create fatty acids and their related derivatives, such as fatty amides, esters, or amines, to carry out several regulatory functions in intracellular and extracellular signaling [60]. Compound **7** produced a molecular ion peak at *m/z* 327.217 $^-$with molecular formula $C_{18}H_{32}O_5$, the deprotonated molecular ions further generated a series of ions at *m/z* 229.1405 [M-H-$C_6H_{10}O$] $^-$and *m/z* 211.1351 [M-H-$C_6H_{10}O$-H_2O]$^-$ was tentatively identified as malyngic acid.

Compound **9** was identified as dimethyl-nonenoic acid (*m/z* 183.1392, $C_{11}H_{20}O_2$). Malyngic acid and dimethyl-nonenoic acid were detected in the DCM fraction only.

Compound **19** with *m/z* 295.228, its molecular formula ($C_{18}H_{33}O_3$) was identified as 13(S)-hydroxy octadecadienoic acid (α-artemisolic acid). Compound **20** (*m/z* 271.2273, $C_{16}H_{32}O_3$) was identified as 2-hydroxy palmitic acid. The negative ion MS spectrum of the unsaturated fatty acid of compound **21** was easy to interpret with exact masses of *m/z* 277.217 as 9,12,15-octadecatrienoic acid (linolenic acid) with molecular formula ($C_{18}H_{30}O_2$). Compounds **19,20 and 21** were detected in Hex. fraction. Compound **22** with a molecular ion peak at*m/z* 471.3827 was identified as 4-methylene-24-ethylsteroid (theonellasterol D). Compound **15**, featuring a precursor ion at m/z 293.2107 [M - H]$^-$, has been tentatively identified as hydroxy-octadecatrienoic acid. The MS/MS spectrum demonstrated typical losses associated with oxylipins, specifically m/z 275 [M – H - H_2O]$^-$ and m/z 231 [M – H - H_2O - CO_2]$^-$. Furthermore, two significant product ions were observed at *m/z* 171 and 121, potentially resulting from the cleavage at the vinylic position adjacent to the hydroxy group [48], [61] . Three lipids (compounds **13,14 and 17**) were tentatively identified as: dihexosylmonoacyl glycerol (18:3), sulfoquinovosylmonoacyl glycerol (18:3), and sulfoquinovosylmonoacyl glycerol (16:0). These identifications were corroborated by the presence of distinct fragment ions, such as the product ions with m/z values of 277 and 255, which are characteristic of octadecatrienoic acid (18:3 fatty acid) and palmitic acid (16:0 fatty acid), respectively [48].

Investigation of the saponifiable matters

The elucidation of the compounds was accomplished by correlating their retention times and fragmentation profiles with those of reference compounds subjected to identical analytical conditions [62], [63],[27].

Table 4: Results of GLC analysis of fatty acids from the lipoidal matterof *L. patersonii* leaves.

Peak	Rt(min)	RR_t	Fatty acids	Carbon no.	Area	Area %
1	2.842	0.167	Caproic acid	C6:0	0.2216	0.04
2	4.778	0.283	Enanthic acid	C7:0	3.5029	0.71
3	4.925	0.290	Caprylic acid	C8:0	2.1754	0.44
4	5.692	0.335	Capric acid	C10:0	0.318	0.06
5	6.805	0.401	Undecanoic acid	C11:0	0.2351	0.05
6	7.118	0.419	Lauric acid	C12:0	0.2176	0.04
7	8.23	0.485	Tridecanoic acid	C13:0	0.4548	0.09
8	9.723	0.573	Myristic acid	C14:0	0.28	0.06
9	9.829	0.579	Myristoleic acid	C14:1	0.5428	0.11
10	9.96	0.587	Pentadecanoic acid	C15:0	0.2105	0.04
11	11.342	0.668	cis-10-pentadecanoic acid	C15:0	0.5529	0.11
12	11.55	0.680	Palmitic acid	C16:0	0.2748	0.06
13	11.651	0.686	Palmetoleic acid	C16:1	0.2507	0.05
14	12.075	0.711	Heptadecanoic acid	C17:0	0.3279	0.07
15	13.118	0.772	cis-10-heptadecanoic acid	C17:0	0.3874	0.08
16	13.541	0.798	Stearic acid	C18:0	0.7558	0.15
17	14.26	0.840	Oleic acid	C18:1	1.4858	0.30
18	14.48	0.853	Eliadic acid	C18:1	0.2894	0.06
19	14.841	0.874	Linoleic acid	C18:2	0.2414	0.05
20	15.364	0.905	Linoleliadic acid	C18:3	0.5552	0.11
21	15.712	0.926	Linolenic acid	C18:3	0.2634	0.05
22	15.946	0.939	gamma-Linolenic acid	C18:3	0.4101	0.08
23	16.083	0.948	Arachidic acid	C20:0	0.3132	0.06
24	16.158	0.952	cis-11-Eicosenoic acid	C20:1	0.2326	0.05
25	16.225	0.956	cis-11,14-Eicosadienoic acid	C20:2	0.2313	0.05

26	16.5	0.972	cis-11,14,17-Eicosatrienoic acid	C20:3	14.116	2.47
27	16.558	0.976	cis-8,11,14-Eicosatrienoic acid	C20:3	0.3418	0.07
28	16.973	1	Arachidonic acid	C20:4	371.4744	74.80
29	17.016	1.003	cis-5,8,11,14,17-Eicosapentaenoic acid	C20:5	93.7582	18.88
30	17.29	1.019	Heneicosanoic acid	C21:0	0.6979	0.14
31	19.068	1.123	Behenic acid	C22:0	0.2224	0.04
32	19.346	1.139	Erucic acid	C22:1	0.4391	0.09
33	19.497	1.1487	cis-13,16-Docosadienoic acid	C22:2	0.2578	0.05

R t= Retention time (min), RRt = Relative retention time (relative to Arachidonic acid; Rt =16.973 min), FA= Fatty acid

Results of GLC analysis of the saponifiable matter of *L. patersonii* leaves (**Table 4**) revealed the presence of 33 fatty acids classified as follows: Unsaturated fatty acids constituted a major part of the total fatty acid composition of the leaves (97.27%). The major unsaturated fatty acid was Arachidonic acid (74.89%). The percentage of saturated fatty acids was (2.24%) in leaves. Enanthic acid was the major detected saturated fatty acid with a relative percentage (0.71%).

Table 5: Identified constituents of unsaponifiable matter (USM) of *L. patersonii* leaves by GLC analysis.

Peak	R_t (min)	RR_t	Identified compound	Carbon no.	Area	Area%
1	6.594	0.3801	*n*-Dodecane	C_{12}	595.085	1.382
2	8.508	0.491	*n*-Tetradecane	C_{14}	244.071	0.567
3	9.798	0.566	*n*-Pentadecane	C_{15}	897.651	2.084
4	11.090	0.641	*n*-Hexadecane	C_{16}	915.934	2.127
5	11.642	0.672	*n*-Heptadecane	C_{17}	1298.071	3.014
6	13.041	0.753	*n*-Octadecane	C_{18}	1657.196	3.848
7	14.601	0.843	*n*-Nonadecane	C_{19}	1828.709	4.246
8	17.313	1	*n*-Eicosane	C_{20}	4604.234	10.690
9	18.594	1.074	*n*-Heneicosane	C_{21}	3918.104	9.097
10	19.516	1.127	*n*-Docsane	C_{22}	2793.020	6.485
11	20.395	1.178	*n*-Tricosane	C_{23}	2044.370	4.747
12	21.247	1.227	*n*-Tetracosane	C_{24}	2095.605	4.866
13	22.064	1.274	*n*-Pentacosane	C_{25}	2609.376	6.059
14	23.417	1.353	*n*-Hexacosane	C_{26}	4467.346	10.373
15	23.866	1.379	*n*-Heptacosane	C_{27}	2153.087	4.999
16	24.121	1.393	Cholesterol	C_{27}	4480.853	10.404
17	25.966	1.499	Stigmasterol	C_{29}	1.513	0.003
18	26.667	1.540	*B*-sitosterol	C_{29}	6238.336	14.485
19	32.308	1.866	*α*-Amyrin	C_{30}	226.254	0.525

Rt=Retention time (min), RRt = Relative retention time (relative to *n*-Eicosane ; Rt = 17.313 min)

Results of GLC analysis of the unsaponifiable matter of *L. patersonii* leaves (**Table 5**) revealed the presence of 19 compounds classified as follows: 15 hydrocarbons (74.584%) and 2 phytosterols (14.488%). Hydrocarbons represented the major portion of the USM of leaves (74.584%), where *n*-Eicosane was the major identified hydrocarbon (10.69%). Sterols constituted about 14.488% of the USM of the leaves. *β*-Sitosterol was the major sterol detected in leaves (14.485%). While *α*-Amyrin (ursane derivative) was the only detected triterpene in USM (0.525%).

Identification and structure elucidation of the isolated compounds from the bioactive fractions

Compound 1 was identified Through ^{1}H NMR, ^{13}C NMR, ESI-MS, HSQC, HMBC, and COSY data by comparing values with the reported literature [64].

24-methylene-3, 4-seco-cycloart-4(28)-en-3-oic acid: MS m/z: $[M+1]^+$ 455. **^{1}H NMR**(400MHz) ($C_{31}H_{50}O_2$) (CDCl3) ppm: δ 2.06 (1H ,m, H-1), 1.35 (1H ,m, H-1), 2.54 (1H ,m, H-2), 2.30 (1H ,m, H-2), 2.43 (1H, *dd*, *j*=12, 5 Hz ,H-5), 1.51 (1H ,m, H-6),1.08 (1H ,m, H-6), 1.31 (1H ,m, H-7), 1.10 (1H ,m, H-7), 1.56 (1H ,m, H-8), 2.15 (1H ,m, H-11), 1.28 (1H ,m, H-11), 1.61 (2H ,m, H-12), 1.30 (2H ,m, H-15), 1.96 (1H ,m, H-16), 1.28 (1H ,m, H-16), 1.61 (1H ,m, H-17), 0.96 (3H ,s, H-18), 0.41 (1H, *d*, *j*=4Hz, H-19), 1.43 (1H, m ,H-20), 0.89 (3H ,*d*, *j*=6.5Hz, H-21), 1.57 (2H,m,H-22), 2.15 (1H, m, H-23), 1.87

(1H,m,H-23), 2.24 (1H,*septet, j*=6.8Hz, H-25), 1.03 (3H,*d, j*=6.8Hz, H-26), 1.04 (3H,*d, j*=6.8Hz, H-27), 4.75 (2H, *brs*, H-28), 1.61 (3H, s, H-29), 0.94 (3H, s, H-30), 4.66 (1H, *brs*, H-31), 4.74 (1H, *brs*, H-31). Some characteristic signals for the compound [cyclopropane methylene at δ 0.41 and 0.74 (*d, j*= 4Hz, H-19), two tertiary methyls at δ 0.94 (H-30) and δ 0.96 (H-18), three secondary methyls at δ 0.90 (*d, j* = 6.5Hz, H-21) and two methyls at δ 1.03(*d, j*=6.8Hz, H-26 and H-27) and one vinyl methyl (δ 1.68, H-29)]

^{13}C NMR (CDCl3, 100MHz) ppm: δ 29.0 (C-1), 31.9 (C-2), 178.4 (C-3), 149.4 (C-4), 45.9 (C-5), 28.0 (C-6), 25.0 (C-7), 47.6 (C-8), 22.0 (C-9), 27.7 (C-10), 28.0 (C-11), 33.0 (C-12), 45.1 (C-13), 48.9 (C-14), 35.6 (C-15), 28.0 (C-16), 52.2 (C-17), 30.3(C-19), 36.1(C-20), 35.6 (C-22),31.9 (C-23),156.9 (C-24), 34.9 (C-25), 22.0 (C-26),111.5 (C-28), 19.7(C-29), 19.3 (C-30),105.9 (C-31).

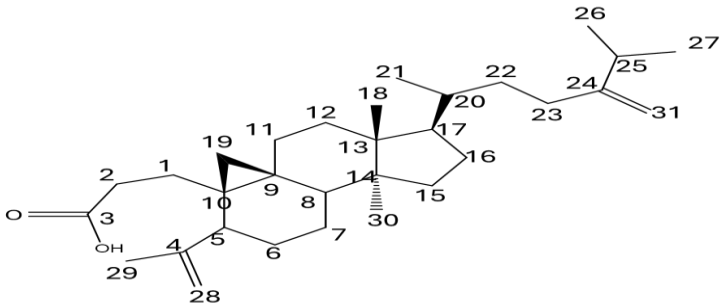

Figure 7: Structure of compound 1 **(**24-methylene-3, 4-seco-cycloart-4(28)-en-3-oic acid)

Compound 2 was identified through^{1}H NMR &^{13}C NMR data by comparing values with the reported literature [65][66].

Triolein^{1}H NMR (400MHz) ($C_{57}H_{104}O_6$) ($CDCl_3$) ppm: δ 5.4 (m, olefinic signals from the fatty acid), δ 5.1 (triplet, glycerol methynic group in sn-2 position), δ 4.2 to δ 4.3 ppm (d, glycerol protons in sn 1,3 position), δ 2.2 ppm (t, methylene groups, α position respecting to carbonylic group); δ 1.9 ppm (m, methylene group in both sides of olefinic protons); δ 1.2 ppm (methylene groups in fatty acid chain); and δ 0.85 ppm (t, terminal CH_3 group).

^{13}C NMR ($CDCl_3$, 100MHz) ppm: δ 175.0 (C-1'), 33.5 (C-2'), 25.5 (C-3'), 29.2 (C-4'), 29.3 (C-5'), 29.7 (C-7'), 26.5 (C-8'), 130.4 (C-10'), 31.8 (C-16'), 22.7 (C-17'), 14.0 (C-18'), 61.7 (C-H_2O).

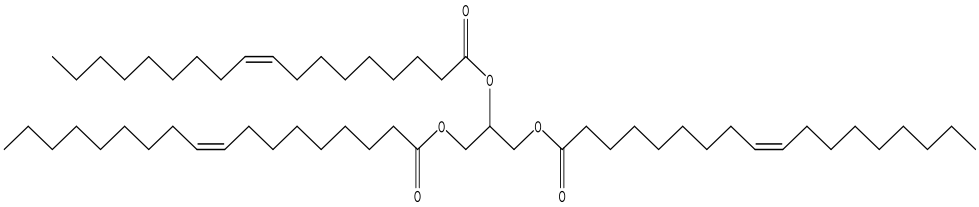

Figure 8: Structure of Compound 2 (Triolein**)**

Compound 3 was identified through ^{1}H NMR by comparing values with the reported literature [67] , [68].

Stigmasterol ^{1}H NMR (400MHz) ($C_{29}H_{48}O$) ($CDCl_3$) ppm: δ3.97 (1H, tdd, J= 4.5, 4.0 and 3.9Hz, H-3), 5.36 (1H, d, J = 5.0Hz, H-6), 1.03 (3H, d, J = 7.0Hz, H-21), 4.25(1H, m, H-22), 5.02 (1H, dd, J= 9.0 and 15.0Hz, H-23) ,2.35(1H, m, H-20), 0.82 (3H, d, J = 7.0Hz, H-26), 0.83 (3H, t, J = 7.0Hz, H-29), 0.84 (3H, d, J = 7.0Hz, H-27). Other peaks are observed at δ 0.76-0.88 (m, 9H), 0.92-1.05 (m, 5H),1.34-1.43 (m, 4H), 0.70-0.73 (m, 3H), 1.8-2.00 (m, 5H), 1.051.13 (m,3H), 1.34-1.63 (m, 9H) ppm. The proton NMR spectrum indicated the following: H-3 appeared as a (tdd) at δ 3.9, olefinic proton signals at δ 5.36 (d), δ 4.25 (m), and 5.02 (dd). The angular methyl protons were observed at δ 1.02 singlet(s) and 0.69 (s) corresponding to the C-18 and C-19 protons, respectively.

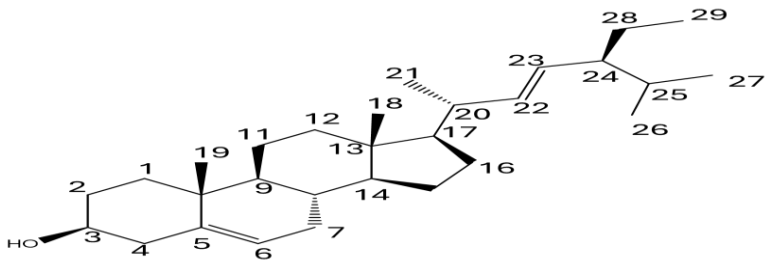

Figure 9: Structure of Compound 3 (Stigmasterol**)**

Some cellular mutations render cells resistant to self-induced death, thus the induction of apoptosis by chemotherapeutic agents is a major target for cancer treatment [69]. Medicinal plants play a pivotal role in both cancer prevention and treatment.

The process of apoptosis begins with cell shrinkage and membrane blebbing, then nucleus fragmentation, and finally, the cell disintegrates into multiple apoptotic bodies [33]. To investigate the cell death induction of the Hex. and DCM fractions of *L. patersonii*extract, fluorescent staining, and immunofluorescence techniques were performed. The findings unequivocally demonstrate that the fractions trigger apoptosis in PC3 cells. The BCL-2 is an early-identified anti-apoptotic protein located on the outer mitochondrial membrane [70].

It effectively prevents apoptosis by blocking mitochondrial permeability pores and inhibiting the release of cytochrome c and apoptosis-inducing factor (AIF). Furthermore, BCL-2 plays a role in inhibiting cell death by modulating caspase activation [71]. Exposure of PC3 cells to half the IC50 dose of Hex. and DCM fractions of *L. patersonii* significantly downregulated the BCL-2 gene. Compounds such as tiliroside, stigmasterol, triolein, and 24-methylene-3,4-seco-cycloart-4(28)-en-3-oic acid demonstrate anti-tumor and cytotoxic properties.

Tiliroside exhibited good cytotoxic activity against PC-3M cell lines [72], as well as stigmasterol exhibits significant cytotoxic activity and holds promise as a novel anticancer agent by suppressing the development of various cancers, including prostate, breast, gastric, hepatoma, skin, and gallbladder cancers [73]. This evidence supports the potential therapeutic applications of stigmasterol in cancer treatment and warrants further investigation.

Previous findings revealed that triolein from Coix seed extract increases p53 protein levels in a concentration-dependent manner in MCF-7 cells. Additionally, triolein enhanced the expression of p53-dependent target genes related to cell cycle arrest, such as p21 and cyclin D1, leading to reduced DNA content. The p53/p21 pathway is crucial in regulating the cell cycle, apoptosis, and cellular stability. Triolein inhibits DNA synthesis in a dose-dependent manner, indicating that it induces cell cycle arrest through the p53/p21 signaling pathway [74].

24-methylene-3,4-seco-cycloart-4(28)-en-3-oic acid exhibited moderate cytotoxic activity against four human tumor cell lines (A549, SK-OV-3, SKMEL-2, and HCT-15) with ED_{50} values of 2.93, 3.01, 3.18 and 2.96 g/mL, respectively [64].

In this study, we investigated the cytotoxic effects of *L. patersonii.* fractions on Caco-2, MCF-7, and PC-3 cancer cell lines using the MTT assay. We screened four fractions (Hex., DCM, EtOAC, and BuOH) against three cell lines and calculated the IC_{50} values. Among the cell lines tested, the PC-3 prostate cancer cell line exhibited the most significant sensitivity to Hex. and DCM fractions, with the lowest IC_{50} values indicating potent cytotoxic effects.

Further investigations into the apoptosis mechanisms revealed that Hex. and DCM fractions induced apoptosis in the PC-3 cell line through the inhibition of BCL-2, a key regulator of cell death. These findings suggest that the plant extracts not only exert cytotoxic effects but also promote apoptosis via BCL-2 inhibition in prostate cancer cells.

UHPLC/QTOF MS/MS, GLC, and isolation were done for the two bioactive fractions. Several compounds were identified in these active fractions. Among these compounds is tiliroside. Also, 3 compounds were isolated from the bioactive fractions through a series of chromatographic techniques (stigmasterol, triolein, and 24-methylene-3,4-seco-cycloart-4(28)-en-3-oic acid). The structures of the isolated compounds were confirmed using spectroscopic methods.

Although the fractions showed repression of BCL2, it was interesting to investigate if the key metabolites have direct interaction with BCL2. A molecular docking study was performed towards the BCL-2 receptor to evaluate the apoptotic potential of the identified and isolated compounds from *L.patersonii*Leaves. Notably, the amino acid residues of the BCL-2 active pocket (Arg103, Arg139, Tyr101, Asn136, and Phe97) were identified to be the crucial ones responsible for the antagonistic activity [75].

Interestingly, one identified (tiliroside) and three isolates (stigmasterol, triolein, and 24-methylene-3,4-seco-cycloart-4(28)-en-3-oic acid) achieved high docking scores (-8.49, -6.09, -10.35, and -6.54 kcal/mol), respectively, compared to the co-crystallized inhibitor of BCL-2 (-9.08 kcal/mol). Their RMSDs were found to be 1.83, 1.31, 1.89, and 1.53 Å, respectively, compared to 1.33 Å of the co-crystallized ligand.

Tiliroside formed one hydrogen bond with Arg103 and one hydrogen-pi bond with Tyr101, however, stigmasterol bound Tyr101 with a hydrogen-pi bond. On the other hand, triolein represented one hydrogen bond with Arg103. Furthermore, 24-methylene-3,4-seco-cycloart-4(28)-en-3-oic acid described one hydrogen bond with Arg139 through an SO_4 bridge (**Figure 10**).

Briefly, the aforementioned high binding scores of the isolated compounds (especially for triolein which exceeded the co-crystallized ligand) recommend greatly the apoptotic potential of the examined candidates from *L.patersonii*Leaves.

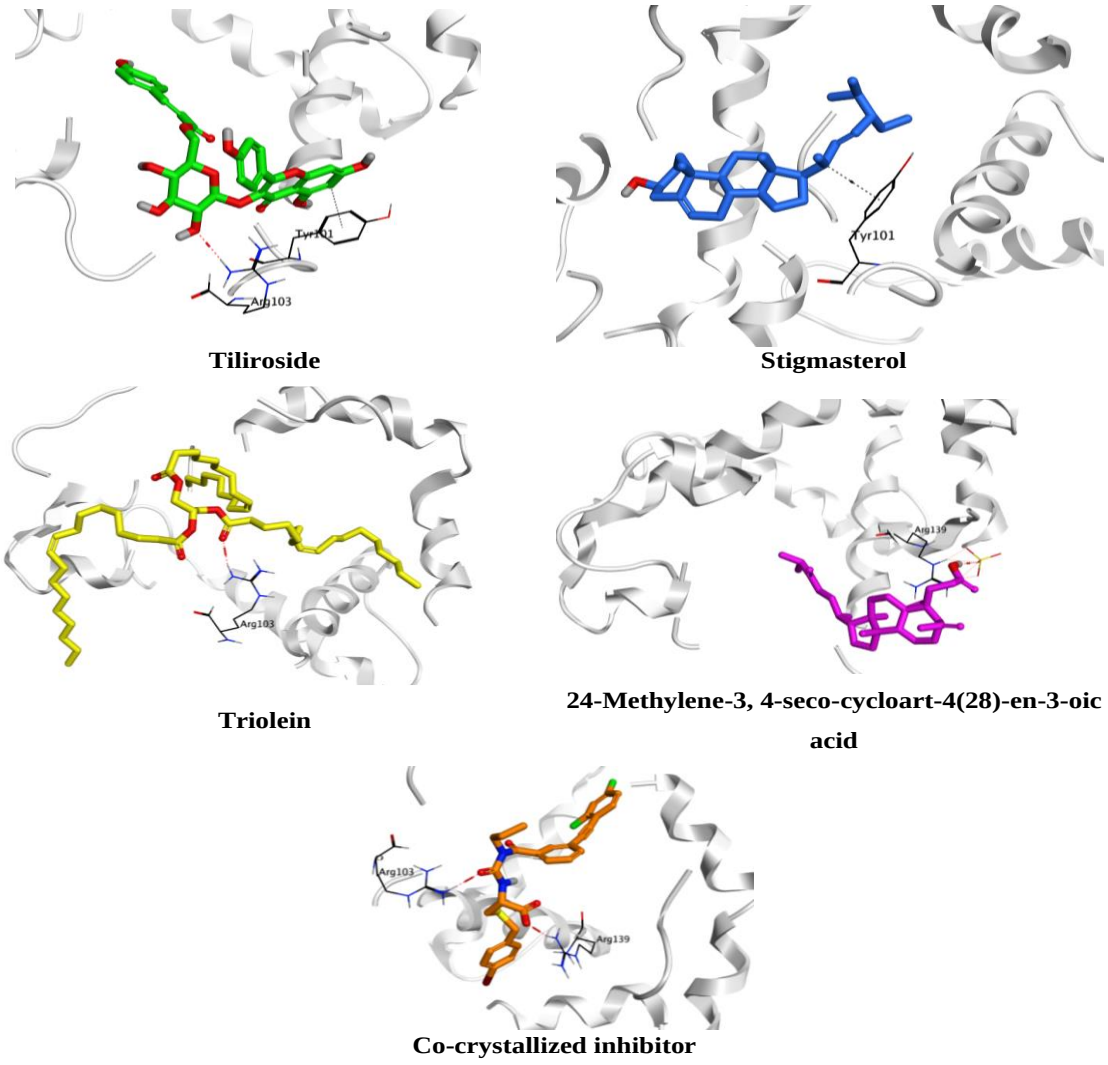

Figure 10. 3D binding interactions of the isolated compounds from *L.patersonii*(Andrews) G. Don. towards the BCL-2 target receptor.

Conclusion

The presence of these compounds in the active fractions suggests that the cytotoxic activity observed in our study may be attributed to their presence. This correlation is further supported by existing literature, which highlights the cytotoxic properties of these compounds. Furthermore, molecular docking showed high binding scores of the isolated compounds (especially for triolein which exceeded the co-crystallized ligand) and recommends greatly the apoptotic potential of the examined candidates from *L.patersonii* Leaves. Further investigation is warranted to confirm the individual and synergistic effects of these compounds in the context of *L. patersonii* extracts and their potential therapeutic applications. The results of our study highlight the potential of plant extracts as promising candidates for the development of novel therapeutic agents targeting prostate cancer. We recommend using the bioactive fractions of *L. patersonii* and/or the isolated compounds as cytotoxic agents instead of using chemotherapy for prostate cancer to benefit from their lesser side effects.

Conflicts of interest

There are no conflicts to declare.

Funding sources

No funding sources

References

[1] J. S. Brown, S. R. Amend, R. H. Austin, R. A. Gatenby, E. U. Hammarlund, and K. J. Pienta, "Updating the Definition of Cancer," *Molecular Cancer Research*, vol. 21, no. 11, pp. 1142-1147, 2023, doi: 10.1158/1541-7786.MCR-23-0411 %J Molecular Cancer Research.

[2] U. T. Sankpal *et al.*, "Environmental factors in causing human cancers: emphasis on tumorigenesis," *Tumor Biology*, vol. 33, pp. 1265-1274, 2012.
[3] S. N. Hart *et al.*, "Mutation prevalence tables for hereditary cancer derived from multigene panel testing," vol. 41, no. 8, pp. e1-e6, 2020.
[4] A. P. de Sousa *et al.*, "In vitro cytotoxicity and ex-vivo genotoxicity in compounds from Waltheria viscosissima A. St. Hil. Brazilian species of the Malvaceae family sensu lato," vol. 51, no. 3, 2022.
[5] M. Thondawada, S. Mulukutla, K. R. S. Raju, S. Dhanabal, and A. J. D. P. C. Wadhwani, "In vitro and In vivo Evaluation of Sida Acuta burm. f.(Malvaceae) for its Anti-oxidant and Anti-Cancer Activity," vol. 8, pp. 396-402, 2016.
[6] D. M Lucas, P. C Still, L. Bueno Perez, M. R Grever, and A. J. C. d. t. Douglas Kinghorn, "Potential of plant-derived natural products in the treatment of leukemia and lymphoma," vol. 11, no. 7, pp. 812-822, 2010.
[7] J. F. Kerr, A. H. Wyllie, and A. R. J. B. j. o. c. Currie, "Apoptosis: a basic biological phenomenon with wideranging implications in tissue kinetics," vol. 26, no. 4, pp. 239-257, 1972.
[8] L. Galluzzi *et al.*, "Cell death modalities: classification and pathophysiological implications," vol. 14, no. 7, p. 1237, 2007.
[9] A. J. Hale *et al.*, "Apoptosis: molecular regulation of cell death," vol. 236, no. 1, pp. 1-26, 1996.
[10] M. M. Hammoud *et al.*, "Synthesis, structural characterization, DFT calculations, molecular docking, and molecular dynamics simulations of a novel ferrocene derivative to unravel its potential antitumor activity," *Journal of Biomolecular Structure and Dynamics*, pp. 1-18, 2022.
[11] A. A. Gaber *et al.*, "Pharmacophore-linked pyrazolo[3,4-d]pyrimidines as EGFR-TK inhibitors: Synthesis, anticancer evaluation, pharmacokinetics, and in silico mechanistic studies," *Archiv der Pharmazie*, vol. n/a, no. n/a, p. e2100258, doi: https://doi.org/10.1002/ardp.202100258.
[12] T. S. Elalfy, N. D. EL Tanbouly, M. E. El-Tantawy, and A. Y. Saleh, "insecticide of plant origin part 1," *Bull. Fac. Pharma. Cairo Univ*, vol. 32, no. 3, pp. 423-426, 1994.
[13] S. Kuppusamy, P. Thavamani, M. Megharaj, R. Nirola, Y. B. Lee, and R. Naidu, "Assessment of antioxidant activity, minerals, phenols and flavonoid contents of common plant/tree waste extracts," *Industrial Crops and Products*, vol. 83, pp. 630-634, 2016.
[14] V. H. Heywood, R. K. Brummitt, A. Culham, and O. Seberg, *Flowering plant families of the world*. Firefly books Ontario, 2007.
[15] C. Pieme, V. Penlap, J. Ngogang, M. J. E. t. Costache, and pharmacology, "In vitro cytotoxicity and antioxidant activities of five medicinal plants of Malvaceae family from Cameroon," vol. 29, no. 3, pp. 223-228, 2010.
[16] M. K. Islam, J. Chowdhury, and I. J. J. o. S. R. Eti, "Biological activity study on a Malvaceae plant: Bombax ceiba," vol. 3, no. 2, pp. 445-450, 2011.
[17] S. M. Razavi, G. Zarrini, G. Molavi, and G. J. I. j. o. b. m. s. Ghasemi, "Bioactivity of Malva sylvestris L., a medicinal plant from Iran," vol. 14, no. 6, p. 574, 2011.
[18] A. E. Sehim *et al.*, "GC-MS analysis, antibacterial, and anticancer activities of Hibiscus sabdariffa L. methanolic extract: In vitro and in silico studies," *Microorganisms*, vol. 11, no. 6, p. 1601, 2023.
[19] V. Harini, "Evaluation of the Anticancer, Antidiabetic, and In vitro Wound Healing Properties of the Aqueous and Ethanolic Extract of Hibiscus rosa-sinensis L," *Journal of Pharmacy and Bioallied Sciences*, vol. 16, no. Suppl 2, pp. S1217-S1222, 2024.
[20] E. Stahl *et al.*, "Adsorbents for TLC," in *Thin-Layer Chromatography: A Laboratory Handbook*: Springer, 1969, pp. 6-52.
[21] T. J. J. I. M. Mosmann, "Use of MTT colorimetric assay to measure cell activation," vol. 65, no. 1, p. 55, 1983.
[22] M. Leite, M. Quinta-Costa, P. S. Leite, and J. E. J. A. C. P. Guimarães, "Critical evaluation of techniques to detect and measure cell death–study in a model of UV radiation of the leukaemic cell line HL60," vol. 19, pp. 139-151, 1999.
[23] A. Bruchmann *et al.*, "Bcl-2 associated athanogene 5 (Bag5) is overexpressed in prostate cancer and inhibits ER-stress induced apoptosis," vol. 13, no. 1, pp. 1-11, 2013.
[24] M. E. Hussein *et al.*, "Anticholinesterase activity of budmunchiamine alkaloids revealed by comparative chemical profiling of two Albizia spp., molecular docking and dynamic studies," *Plants*, vol. 11, no. 23, p. 3286, 2022.
[25] T. Pluskal, S. Castillo, A. Villar-Briones, and M. J. B. b. Orešič, "MZmine 2: modular framework for processing, visualizing, and analyzing mass spectrometry-based molecular profile data," vol. 11, no. 1, pp. 1-11, 2010.
[26] I. Vogel, *Practical organic chemistry*. Citeseer, 1974.
[27] R. Farag, A. Ahmed, S. Rashad, and M. Ewies, "Unsaponifiable matter of six pollens collected by honeybees in Egypt," *Journal of Apicultural Research*, vol. 19, no. 4, pp. 248-254, 1980.
[28] R. Huey, G. M. Morris, and S. Forli, "Using AutoDock 4 and AutoDock vina with AutoDockTools: a tutorial," *The Scripps Research Institute Molecular Graphics Laboratory*, vol. 10550, no. 92037, p. 1000, 2012.
[29] S. Yuan, H. S. Chan, and Z. Hu, "Using PyMOL as a platform for computational drug design," *Wiley Interdisciplinary Reviews: Computational Molecular Science*, vol. 7, no. 2, p. e1298, 2017.
[30] O. Kutkat *et al.*, "Robust antiviral activity of commonly prescribed antidepressants against emerging coronaviruses: in vitro and in silico drug repurposing studies," *Scientific Reports*, vol. 12, no. 1, p. 12920, 2022/07/28 2022, doi: 10.1038/s41598-022-17082-6.
[31] M. A. Salem, N. M. Aborehab, A. A. Al-Karmalawy, A. R. Fernie, S. Alseekh, and S. M. Ezzat, "Potential Valorization of Edible Nuts By-Products: Exploring the Immune-Modulatory and Antioxidants Effects of Selected

Nut Shells Extracts in Relation to Their Metabolic Profiles," *Antioxidants*, vol. 11, no. 3, p. 462, 2022. [Online]. Available: https://www.mdpi.com/2076-3921/11/3/462.

[32] M. A. Aziz, W. S. Shehab, A. A. Al-Karmalawy, A. F. EL-Farargy, and M. H. Abdellattif, "Design, Synthesis, Biological Evaluation, 2D-QSAR Modeling, and Molecular Docking Studies of Novel 1H-3-Indolyl Derivatives as Significant Antioxidants," *International Journal of Molecular Sciences*, vol. 22, no. 19, p. 10396, 2021. [Online]. Available: https://www.mdpi.com/1422-0067/22/19/10396.

[33] A. Mohammadi, B. Mansoori, M. Aghapour, and B. Baradaran, "Urtica dioica dichloromethane extract induce apoptosis from intrinsic pathway on human prostate cancer cells (PC3)," *Cellular and Molecular Biology*, vol. 62, no. 3, pp. 78-83, 2016.

[34] S. K. Pal and Y. Shukla, "Herbal medicine: current status and the future," *Asian pacific journal of cancer prevention*, vol. 4, no. 4, pp. 281-288, 2003.

[35] S. HemaIswarya and M. Doble, "Potential synergism of natural products in the treatment of cancer," *Phytotherapy Research: An International Journal Devoted to Pharmacological and Toxicological Evaluation of Natural Product Derivatives*, vol. 20, no. 4, pp. 239-249, 2006.

[36] H. Tamaki *et al.*, "Bcl-2 family inhibition sensitizes human prostate cancer cells to docetaxel and promotes unexpected apoptosis under caspase-9 inhibition," vol. 5, no. 22, p. 11399, 2014.

[37] C. Xia *et al.*, "Comprehensive profiling of macamides and fatty acid derivatives in maca with different postharvest drying processes using UPLC-QTOF-MS," *ACS omega*, vol. 6, no. 38, pp. 24484-24492, 2021.

[38] R. E. March, E. G. Lewars, C. J. Stadey, X.-S. Miao, X. Zhao, and C. D. J. I. J. o. M. S. Metcalfe, "A comparison of flavonoid glycosides by electrospray tandem mass spectrometry," vol. 248, no. 1-2, pp. 61-85, 2006.

[39] Y. Chen *et al.*, "Characterization and Quantification by LC-MS/MS of the Chemical Components of the Heating Products of the Flavonoids Extract in Pollen Typhae for Transformation Rule Exploration," vol. 20, no. 10, pp. 18352-18366, 2015. [Online]. Available: https://www.mdpi.com/1420-3049/20/10/18352.

[40] T. Beelders, D. De Beer, M. A. Stander, and E. Joubert, "Comprehensive phenolic profiling of Cyclopia genistoides (L.) Vent. by LC-DAD-MS and-MS/MS reveals novel xanthone and benzophenone constituents," *Molecules*, vol. 19, no. 8, pp. 11760-11790, 2014.

[41] K. Wang *et al.*, "Identification of components in Citri Sarcodactylis Fructus from different origins via UPLC-Q-Exactive Orbitrap/MS," *ACS omega*, vol. 6, no. 26, pp. 17045-17057, 2021.

[42] A. Pascoal, R. Quirantes-Piné, A. L. Fernando, E. Alexopoulou, A. J. I. C. Segura-Carretero, and Products, "Phenolic composition and antioxidant activity of kenaf leaves," vol. 78, pp. 116-123, 2015.

[43] Q. Wang *et al.*, "Using Identification and Quantification to Decipher The Dynamic Changes of Main Chemical Components In The Processing of Stir-Frying Codonopsis Radix With Rice By HPLC-MS/MS," *Research Square*, 2020.

[44] U. A. Fischer, R. Carle, and D. R. Kammerer, "Identification and quantification of phenolic compounds from pomegranate (Punica granatum L.) peel, mesocarp, aril and differently produced juices by HPLC-DAD–ESI/MSn," *Food chemistry*, vol. 127, no. 2, pp. 807-821, 2011.

[45] V. Agme-Ghodke, R. N. Agme, and A. Sagar, "Analysis of bioactive compounds in leaves extract of Centella asiatica by using HRLC-MS & IR techniques," *Journal of Chemical Pharmaceutical Research*
vol. 8, no. 8, pp. 122-125, 2016.

[46] R. Gil-Solsona *et al.*, "Metabolomic approach for Extra virgin olive oil origin discrimination making use of ultra-high performance liquid chromatography–Quadrupole time-of-flight mass spectrometry," *Food Control*, vol. 70, pp. 350-359, 2016.

[47] C. Xia *et al.*, "Evaluation of the Antioxidant Potential of Citrus medica from Different Geographical Regions and Characterization of Phenolic Constituents by LC–MS," vol. 8, no. 36, pp. 32526-32535, 2023.

[48] A. M. Otify *et al.*, "Unveiling metabolome heterogeneity and new chemicals in 7 tomato varieties via multiplex approach of UHPLC-MS/MS, GC–MS, and UV–Vis in relation to antioxidant effects as analyzed using molecular networking and chemometrics," *Food Chemistry*, vol. 417, p. 135866, 2023.

[49] U. Khurshid *et al.*, "Phytochemical composition and in vitro pharmacological investigations of Neurada procumbens L.(Neuradaceae): A multidirectional approach for industrial products," *Industrial Crops and Products*, vol. 142, p. 111861, 2019.

[50] A. Soria-Lopez *et al.*, "Metabolic profiling via UPLC/MS/MS and in vitro cholinesterase, amylase, glucosidase, and tyrosinase inhibitory effects of Carica papaya L. extracts reveal promising nutraceutical potential," *Food Analytical Methods*, vol. 18, no. 1, pp. 57-74, 2025.

[51] I. M. Abu-Reidah, M. S. Ali-Shtayeh, R. M. Jamous, D. Arráez-Román, and A. J. F. R. I. Segura-Carretero, "Comprehensive metabolite profiling of Arum palaestinum (Araceae) leaves by using liquid chromatography–tandem mass spectrometry," vol. 70, pp. 74-86, 2015.

[52] G. H. Attia, D. A. Marrez, M. A. Mohammed, H. A. Albarqi, A. M. Ibrahim, and M. A. E. Raey, "Synergistic effect of mandarin peels and hesperidin with sodium nitrite against some food pathogen microbes," *Molecules*, vol. 26, no. 11, p. 3186, 2021.

[53] Y. Gao and S. Wu, "Comprehensive analysis of the phospholipids and phytosterols in Schisandra chinensis oil by UPLC-Q/TOF-MSE," *Chemistry physics of lipids*

vol. 221, pp. 15-23, 2019.

[54] V. J. I. J. o. G. P. Vadivel, "Distribution of flavonoids among Malvaceae family members–A review," vol. 10, no. 1, 2016.
[55] U. Saleem *et al.*, "Neuroprotective potential of Malva neglecta is mediated via down-regulation of cholinesterase and modulation of oxidative stress markers," vol. 36, pp. 889-900, 2021.
[56] M. S. Oliveira *et al.*, "Chemical constituents, antioxidant and antimicrobial activities of Pavonia glazioviana Gurke (Malvaceae)," *Química Nova,* vol. 48, no. 1, pp. e-20250011, 2024.
[57] A. Singh, S. Kumar, V. Bajpai, T. J. Reddy, K. Rameshkumar, and B. Kumar, "Structural characterization of flavonoid C-and O-glycosides in an extract of Adhatoda vasica leaves by liquid chromatography with quadrupole time-of-flight mass spectrometry," *Rapid Communications in Mass Spectrometry,* vol. 29, no. 12, pp. 1095-1106, 2015.
[58] G. Das *et al.*, "Systematics, phytochemistry, biological activities and health promoting effects of the plants from the subfamily bombacoideae (family Malvaceae)," *Plants,* vol. 10, no. 4, p. 651, 2021.
[59] N. M. Mohammed, A. M. Kamal, M. I. Abdelhady, and E. G. J. J. o. A. P. R. Haggag, "HPLC Phenolic Profiling of Alcoholic Extracts of Three Abutilon Species," vol. 5, no. 4, pp. 371-376, 2021.
[60] H. Weber, "Fatty acid-derived signals in plants," *Trends in plant science*
vol. 7, no. 5, pp. 217-224, 2002.
[61] P. Wheelan, J. A. Zirrolli, and R. C. Murphy, "Low-energy fast atom bombardment tandem mass spectrometry of monohydroxy substituted unsaturated fatty acids," *Biological mass spectrometry,* vol. 22, no. 8, pp. 465-473, 1993.
[62] F. Fryer, W. Ormand, and G. Crump, "Triglyceride elation by gas chromatography," 1960.
[63] J. Nelson and A. Milun, "Gas chromatographic determination of tocopherols and sterols in soya sludges and residues," *Journal of the American Oil Chemists' Society,* vol. 45, no. 12, pp. 848-851, 1968.
[64] H. J. Kim *et al.*, "A cytotoxic secocycloartenoid from Abies koreana," *Archives of pharmacal research,* vol. 24, pp. 527-531, 2001.
[65] M. F. Díaz, J. A. Gavín, and J. B. De Andrade, "Structural characterization by Nuclear Magnetic Resonance of ozonized triolein," *Grasas y aceites,* vol. 59, no. 3, pp. 274-281, 2008.
[66] L. Mannina, C. Luchinat, M. Patumi, M. C. Emanuele, E. Rossi, and A. J. M. R. i. C. Segre, "Concentration dependence of 13C NMR spectra of triglycerides: implications for the NMR analysis of olive oils," vol. 38, no. 10, pp. 886-890, 2000.
[67] A. Kamboj and A. K. Saluja, "Isolation of stigmasterol and β-sitosterol from petroleum ether extract of aerial parts of Ageratum conyzoides (Asteraceae)," *Int. J. Pharm. Pharm. Sci,* vol. 3, no. 1, pp. 94-96, 2011.
[68] J. M. Amaro-Luis, A. Duque-Márquez, P. Ramoni-Perazzi, and M. Muñoz-Romo, "Isolation and characterization of stigmasterol from highly consumed leaves by the large fruit-eating bat, Artibeus amplus (Chiroptera: Phyllostomidae)," *Interciencia,* vol. 46, no. 9/10, pp. 363-368, 2021.
[69] O. Ait-Mohamed *et al.*, "Acetonic extract of Buxus sempervirens induces cell cycle arrest, apoptosis and autophagy in breast cancer cells," *PloS one,* vol. 6, no. 9, p. e24537, 2011.
[70] H. Hu, N. S. Ahn, X. Yang, Y. S. Lee, and K. S. Kang, "Ganoderma lucidum extract induces cell cycle arrest and apoptosis in MCF-7 human breast cancer cell," *International Journal of Cancer,* vol. 102, no. 3, pp. 250-253, 2002.
[71] H. R. Horvitz, "Worms, life, and death (Nobel lecture)," *Chembiochem,* vol. 4, no. 8, pp. 697-711, 2003.
[72] S. Sameh *et al.*, "Family Malvaceae: a potential source of secondary metabolites with chemopreventive and anticancer activities supported with in silico pharmacokinetic and pharmacodynamic profiles," *Frontiers in Pharmacology,* vol. 15, p. 1465055, 2024.
[73] N. P. Dube *et al.*, "In vitro cytotoxic effect of stigmasterol derivatives against breast cancer cells," *BMC Complementary Medicine and Therapies,* vol. 23, no. 1, p. 316, 2023.
[74] T. T. Hien, L. V. Duc, T. T. Dao, and N. T. Hai, "Triolein from Coix Lacryma-Jobi induces cell cycle arrest through p53/p21signaling pathway," *Biomedical and Pharmacology Journal,* vol. 9, no. 2, pp. 519-524, 2016.